PROCEEDINGS of the
23rd International Congress on Acoustics

9 to 13 September 2019 in Aachen, Germany

Outer wall inspection by noncontact acoustic inspection method using sound source mounted type UAV

Tsuneyoshi SUGIMOTO[1]; Kazuko SUGIMOTO[2]; Itsuki UECHI[3];
Noriyuki UTAGAWA[4]; Chitose KURODA[5]

[1-3] Graduate School of Engineering, Toin University of Yokohama, Japan

[4-5] Technical Research Institute SatoKogyo Co. Ltd., Japan

ABSTRACT

By using the noncontact acoustic inspection method that utilizes flexural resonance generated by acoustic irradiation induced vibration, crack defect existing near the surface of the measurement target can be non-destructively inspected from a long distance. It has been proved that the same test as the hammering test can be done with tunnels and bridges with a height of over 30 m and shotcrete with a rough surface. This method has problems such as environmental noise and angle dependency. However, when a sound source itself is mounted on an unmanned aerial vehicle (UAV) which is becoming popular in recent years, it becomes possible to make the sound source position directly face the measurement target surface, and these problems are expected to be resolved. Therefore, we investigated outer wall inspection by noncontact acoustic inspection method using sound source mounted type UAV. The inspection results using the outer wall specimen were good, and it became clear that peel defects of the tile can be detected even with a small sound source that can be mounted on UAV.

Keywords: Non-destructive inspection, Noncontact acoustic inspection, Sound source mounted type UAV

1. INTRODUCTION

1.1 Background

The collapse of the Morandi bridge in Genova, which occurred in August 2018, was shocking. However, visual inspection or hammering test method are still used as inspection methods for the outer wall of a building and a concrete structure. As a quantitative nondestructive inspection method, an impact echo method (1,2), an ultrasonic inspection method (3,4), an electromagnetic inspection method (5) and an impact acoustics method (6) have already been developed. However, these techniques require contact or nearly contact with the measurement surface. As a result, temporary scaffolding is necessary, and improvement of workability beyond the hammering test cannot be expected. Therefore, development of a long distance noncontact inspection method is required.

1.2 Long distance noncontact inspection method

As a long-distance noncontact inspection method, impact exploration method (7) by pressure wave using gas gun and water hammer exploration method (8) using water gun have been proposed. However, the former has a problem in continuous measurement, and the latter has a problem that a large amount of water is required. On the other hand, if an infrared camera is used, it is possible to measure the temperature distribution of the object surface without contact (9). However, in a tunnel where temperature change is small, heating such as a heater is required at the time of detection, so it is not suitable for high ceiling exploration. In addition, since the measurement results show only the influence of temperature change near the surface, it seems to be insufficient in principle as an

[1] tsugimot@toin.ac.jp
[2] kazukosu@toin.ac.jp
[3] iuechi84@toin.ac.jp
[4] utagawa@satokogyo.co.jp
[5] kuroda@satokogyo.co.jp

alternative to the hammer method. Furthermore, laser ultrasonic method (10) using laser irradiation induced vibration is also a method that can remotely detect defects, and it seems to be particularly suitable for inspection of metals having a high melting point. However, in the case of outer wall tiles and concrete, since the melting point is low, only a very short time of laser irradiation can be performed so as not to damage the surface. Therefore, there is a disadvantage that it is not possible to add effective vibrational energy commensurate with high power. In addition, problems with safety due to using multiple high-power lasers have been pointed out. In recent years, a method using noncontact airborne ultrasound has also been proposed. Extremely high sound pressure can be generated by focusing on ultrasound (11). However, due to the large propagation attenuation in the air, it seems difficult to be practically used for the actual structure.

1.3 Noncontact acoustic inspection method using acoustic irradiation induced vibration

Therefore, we proposed a noncontact acoustic inspection (NCAI) method to detect the flexural resonance due to the acoustic irradiation induced vibration with a laser Doppler vibrometer (LDV). And it has been shown that void defects in concrete specimens can be detected even from a distance of 5m or more (12). Then, in order to improve practical defect detection performance, single tone burst wave (13), vibration energy ratio (14) and defect detection algorithm using spectral entropy (15,16) were devised. We also devised multitone burst wave (17) that enable faster measurement and spatial spectral entropy (18) for separating and detecting defects and head resonance of LDV. In addition, it has been shown that defect detection equivalent to hammering test can be performed by an actual railway tunnel, a high bridge over 30 m (19) and a shotcrete with rough surface (20,21). However, the problems of this method were angular dependence of sound source and environmental noise. Here, the angle dependence means that the defect detection capability becomes lower as the irradiation angle of the acoustic wave becomes larger. The reason for this is that it becomes difficult to generate flexural vibration when it is impossible to apply a uniform surface excitation force.

1.4 NCAI method using sound source mounted type UAV

On the other hand, an unmanned aerial vehicle (UAV), so-called drone with multiple rotors has become available for aerial photography in recent years (22). It is already used for crack inspection etc. which can be confirmed from the surface. In the NCAI method, angle dependence and environmental noise were problems, but in reality these are problems caused by the sound source. However, if the sound source itself is mounted on the UAV and it is possible to irradiate the acoustic wave from near the measured object, it is assumed that these problems will be solved. In other words, since the sound source mounted type UAV can make the sound source face directly on the measurement target surface, it can be predicted that the problem of the angle dependency is solved. In addition, since the sound source itself can be brought close to the surface to be measured, measurement with a small sound source becomes possible, and environmental noise can also be expected to resolve spontaneously. Furthermore, the application range of this method can be expanded to the distance up to the measurable limit of LDV, and as the position of the LDV and the sound source are away from each other, the resonance problem of the LDV head is also solved, high speed measurement can be expected. Therefore, in order to solve the problem of the NCAI method and expand the range of application, we examined the outer wall inspection by the NCAI method using sound source mounted type UAV.

2. Sound source mounted type UAV and outer wall specimen

2.1 Sound source mounted type UAV (prototype)

Figure 1 shows an external view of the sound source mounted type UAV (prototype). The base body is DJI's Matrice 600 Pro, which is equipped with a flat speaker (FPS Corp., 1030M3F1R), a sighting laser pointer and a laser rangefinder on the underside of the UAV body. The weight of the UAV itself is about 10 kg, and it can fly for about 20 minutes with a sound source and an amplifier. In addition, the waveform for acoustic irradiation induced vibration can be transmitted by wireless communication, and it can be synchronized with the measurement on the LDV side.

2.2 Tiled outer wall specimen

A tiled outer wall specimen ($2 \times 1.0 \times 0.2$ m^3 $+2 \times 0.6 \times 0.6$ m^3) was made for verification experiments on outer wall inspection using UAV (The bottom part is thickened because it simulates

the pillar part). The overview photograph is shown in Fig. 2 (a). Because the weight is about 2.6 tons, wheels are attached to the bottom of the specimen to facilitate movement. The layout of the simulated defective sheets embedded in the specimen are shown in Fig. 2 (b). Various sizes of styrene sheets of thickness 0.5 mm and foamed sheets of 1 mm thickness were used as simulated cracks. The burial depth of the sheet is about 9 mm from the tile surface, assuming that the thickness from the concrete base material to the top surface of the tile is 10 mm. The size of one tile is about 45 × 95 mm^2. The same simulated defects are attached to the upper and lower two stages, but the difference is the thickness of the concrete wall. The top two rows are placed on concrete walls about 20 cm thick and the bottom two rows are placed on concrete walls about 60 cm thick simulating pillars. However, this difference in thickness had no particular effect on the experimental results. From the visual appearance it is completely unknown where the defects are.

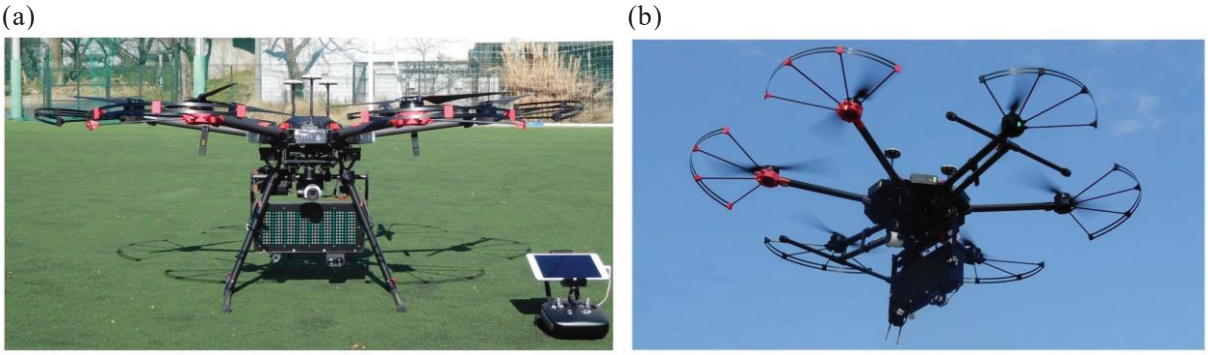

Figure 1 –Photographs of the sound source mounted type UAV (prototype).
(a) At the time of the ground, (b) At the time of flight.

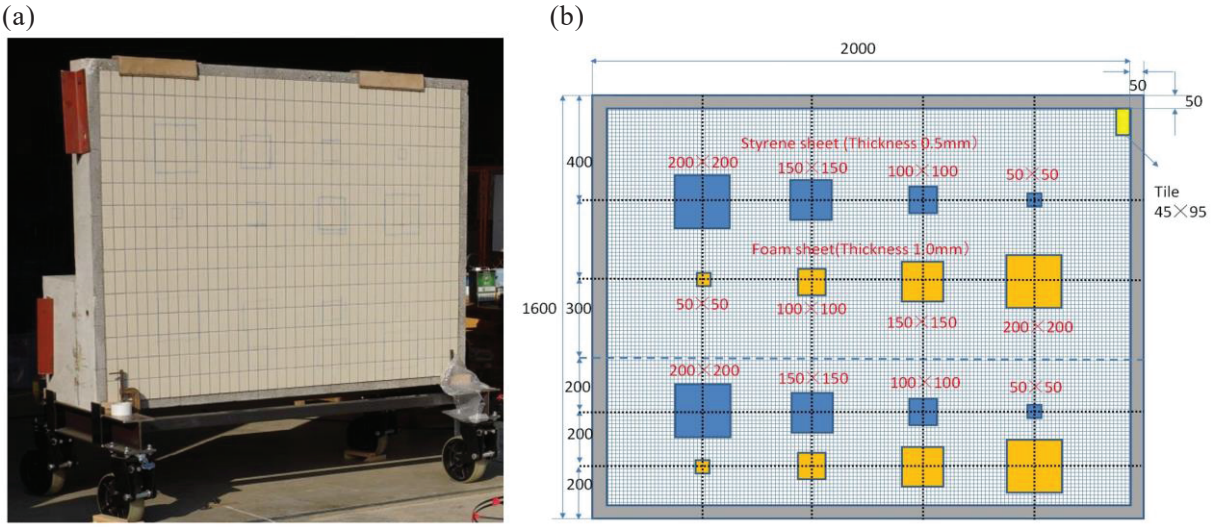

Figure 2 – A tiled outer wall specimen (2×1.0×0.2 m^3+2×0.6×0.6 m^3). (a) Overview picture, (b) Arrangement of simulated defect sheet (depth is about 9 mm). Various sizes of styrene sheets of thickness 0.5 mm and foamed sheets of 1 mm thickness were used as simulated cracks.

3. Acoustic irradiation experiment

The following three experiments were conducted to confirm the effectiveness of the NCAI method by acoustic irradiation induced vibration from sound source mounted type UAV to an outer wall specimen.

- Experiment I : When the acoustic wave is irradiated in front of a simulated defect.
- Experiment II : When the acoustic wave is irradiated to the center of the specimen.
- Experiment III: When the acoustic wave is irradiated during UAV flight at very low attitudes.
- Experiment IV: When the acoustic wave is irradiated during UAV flight at about 4m height.

3.1 Experiment I

3.1.1 Experimental setup

Firstly, verification experiment was carried out with the sound source facing simulated defects. Therefore, the UAV was mounted on the rear part of the transportation vehicle (actually there is a reason that the strong wind was blowing and it was not able to fly). Acoustic irradiation experiment was carried out on eight topside simulated defects (defect size 50 to 200 mm^2) of the outer wall specimen. An experimental setup in Experiment I is shown in Fig. 3(a). The distance between the sound source and the outer wall specimen was about 1.6 to 1.7 m. The vibration velocity distribution around the defect positions were measured using a scanning laser Doppler vibrometer (SLDV: Polytec Corp., PSV-500 Xtra) which can measure the surface vibration velocity distribution. Because the rear part of the transportation vehicle was near the specimen, the SLDV was moved to a position that was easy to measure due to the defect position. Therefore, the distance between the SLDV and the specimen is about 2.4 to 3.4 m, the laser incident angle was about 38° to 55° when vertical incidence was 0°. The waveform used for acoustic irradiation was a single tone burst (STNB) wave (17), and two kinds of waveforms were created and used to match the flexural resonance frequency of the target defect. The first waveform was used when the defect size was 100 to 200 mm^2, and the frequency range was 0.5 to 4 kHz. The second waveform was used when the defect size was 50 mm^2, and the frequency range was 9 to 13 kHz. Both waveforms have a pulse width of 5 ms (modulation frequency was 100 Hz), and the emission interval of each pulse was 15 ms. The sound pressure at the time of excitation was set to about 95 dB (the maximum value of the Z characteristic) near the measurement target surface.

3.1.2 Experimental result

An example of the result based on the vibration energy ratio in the frequency band used is shown in Fig. 3(b). The frequency range for calculating the vibration energy ratio (14) is 0.5 to 4 kHz when the size of the defect is 100 to 200 mm^2, 9 to 13 kHz when it is 50 mm^2 according to the emission waveform. The number of measurement points was 121 (11 × 11), and the measurement time was about 9 minutes 11 seconds when the addition average was 5 times. It can be seen from this figure that all defect sizes of 50 to 200 mm^2 are detected. Among them, 50 mm^2 defects have a high flexural resonance frequency as high as 10 kHz or more, so it is a difficult defect to be found by normal hammering test.

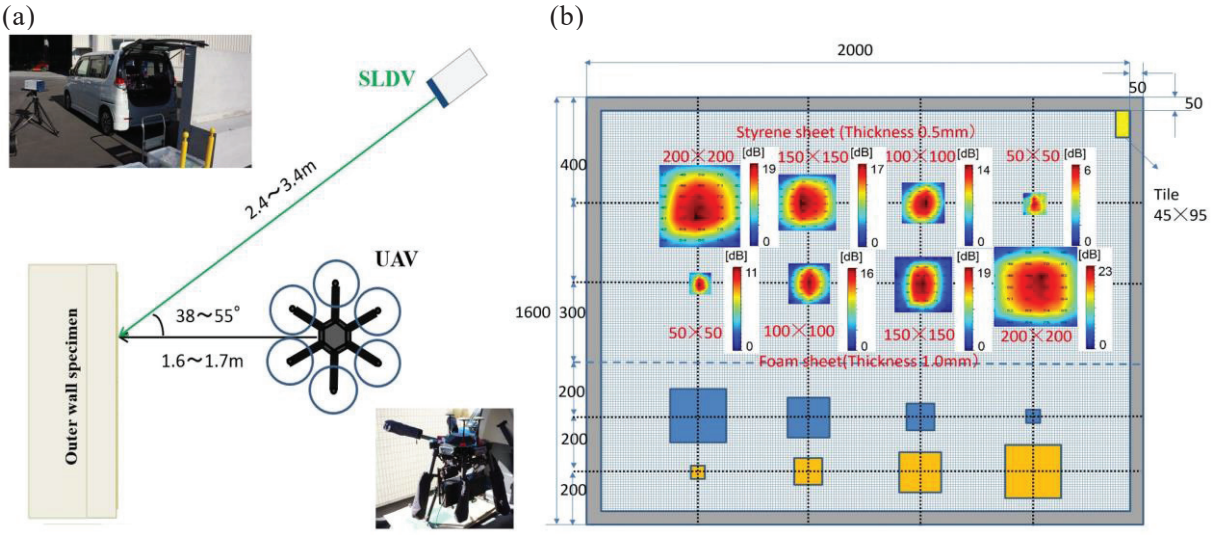

Figure 3 –Experiment when the acoustic wave is irradiated in front of a simulated defect.
(a) Experimental setup, (b) Experimental result using vibrational energy ratio. The integration range is 500-4000 Hz for 100 - 200 mm^2, 9 - 13 kHz for 50 mm^2. All simulated defects can be detected.

3.2 Experiment II

3.2.1 Experimental setup

When the UAV actually fly, it is expected that the UAV itself will swing due to the influence of wind etc. However, in the case of acoustic irradiation induced vibration, even if the sound source

cannot be accurately confronted with the defect position, the measurement itself is considered to be possible if it is within the directivity range of the sound source. The flat speaker mounted on the UAV has a directivity of about 30 degrees at 4 kHz according to the manufacturer's published datasheet. Therefore, if the distance is about 3 m, it is possible to irradiate acoustic waves with frequencies of 4 kHz or less for all the front surface of the outer wall specimen. Therefore, a verification experiment was conducted in the case where the acoustic wave was irradiated to the central part of the outer wall specimen next. Figure 4(a) is a photograph showing the arrangement of the equipment during the experiment. For indoor experiment, an UAV was placed on a table, and the distance between a sound source and an outer wall specimen was about 3 m. The distance between a SLDV (Polytec Corp., PSV-500 Xtra) and an outer wall specimen was about 4.3 m and it was placed somewhat diagonally behind the sound source. As the irradiation acoustic wave, a multitone burst (MTNB) wave (17) having a frequency range of 0.3 to 4 kHz was used. In this waveform, 38 frequencies of pulse width 5 ms (modulation frequency was 100 Hz) were included, and the total time length was about 197 ms. In order to scan the front of the specimen at high speed, by setting the emission interval (200ms) to be slightly longer than the whole length of the waveform, all frequencies were sent with one emission and the average processing was not performed.

3.2.2 Experimental result

The scan area size was set at about 4.5 cm intervals in the area of about 130 × 153 cm^2, and the number of measurement points was set to 1015 (29 × 35) points. The sound pressure was set to be about 95 dB (the maximum value of the Z characteristic) near the measurement target surface, and the measurement time was about 7 minutes (about 0.4 seconds per point). Figure 4(b) shows the distribution of vibration energy ratio integrated over the range of 0.3 to 4 kHz. The white frames show the size and position of the defect parts. It can be seen that 50 mm^2 with high resonance frequency is not detected due to the emission frequency range, but other defects are almost detected. The reason that the noise is slightly conspicuous is that, in addition to the condition that there was no average, the position of the laser head and the sound source were not apart from each other in the closed environment, it seems that it was influenced by the reflected sound from the specimen and the multiple reflected sounds from the surroundings.

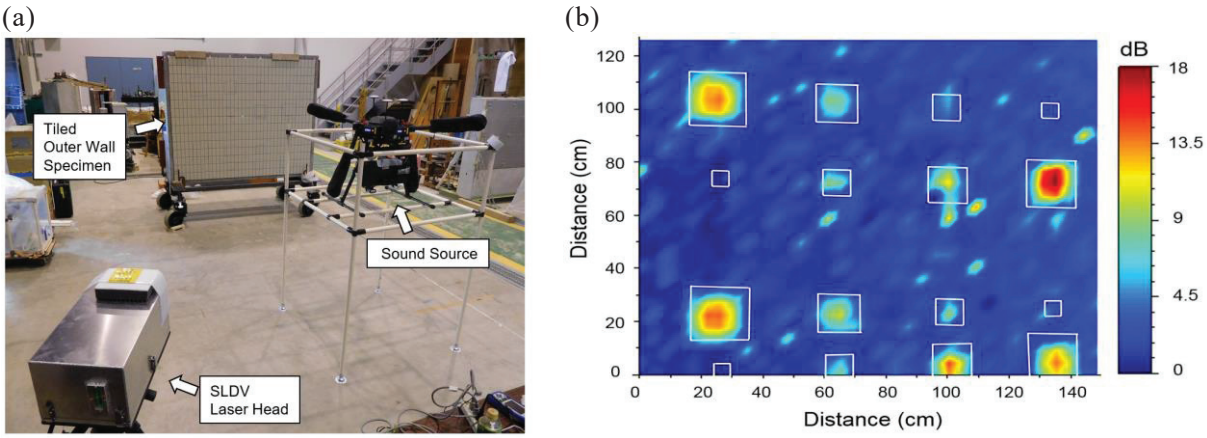

Figure 4 –Experiment when the acoustic wave is irradiated at the center of the outer wall specimen. (a) A photograph of the experimental setup, (b) An example of the experimental result using vibrational energy ratio (300-4000Hz).

3.3 Experiment III

3.3.1 Experimental setup

An experiment was conducted to make the UAV with sound source actually fly outdoors and explore the outer wall specimen. An experiment setup is shown in Fig. 5(a). As shown in this figure, the UAV flew so that it faced the specimen. The flight height was set to about 2 m according to the height including the truck of the specimen so that the distance between the sound source and the specimen was about 2 to 3 m. The reason why this distance is ambiguous is that the UAV itself swings during flight. In other words, since the height is as low as about 2 m, the wind taken up by the multiple rotors returns to the UAV itself from the ground. Also, SLDV (Polytec Corp., PSV-500 Xtra) was

placed at a position about 3.8 m diagonally backward to avoid the influence of reflected wave. The resonance phenomenon of the laser head due to the reflected wave does not occur in principle when the SLDV is away from the sound axis with strong sound pressure. Furthermore, it can be expected that the signal to noise ratio also improves if there is no influence of multiple reflection sound etc. from the surroundings by outdoor experiments. For this reason, continuous irradiation of the MTNB wave with a shorter pulse width was carried out in order to check whether measurement faster than the previous section is possible (Frequency range; 0.5 to 4 kHz, pulse width; 3 ms (modulation frequency; 200 Hz), waveform overall length; about 59 ms, and emission interval; 60 ms). In addition, the sound pressure was about 90 to 95 dB (maximum value of Z characteristic) near the measurement target surface.

3.3.2 Experimental result

The measured object was a 200 mm^2 styrene sheet placed on the upper left of the specimen. Figure 5(b) shows an example of the image result by vibration energy ratio (0.5-2.4 kHz). The white frame shows the size and position of the measured object. From this figure, it was confirmed that although the UAV itself swayed a little during the experiment, even if the irradiation of the acoustic wave was in a short time, the defect could be detected if it was in the directivity range of the sound source. Since the number of measurement points was 81 (scan area size; 32 × 32 cm^2, scan pitch; 4 cm), the measurement time was only 21 seconds. This means that only about 0.26 seconds were needed per point for this measurement. In addition, since the frequency band of the wind noise by the multiple rotors was low frequency of 100-200 Hz, it was easily removed by the low cut filter.

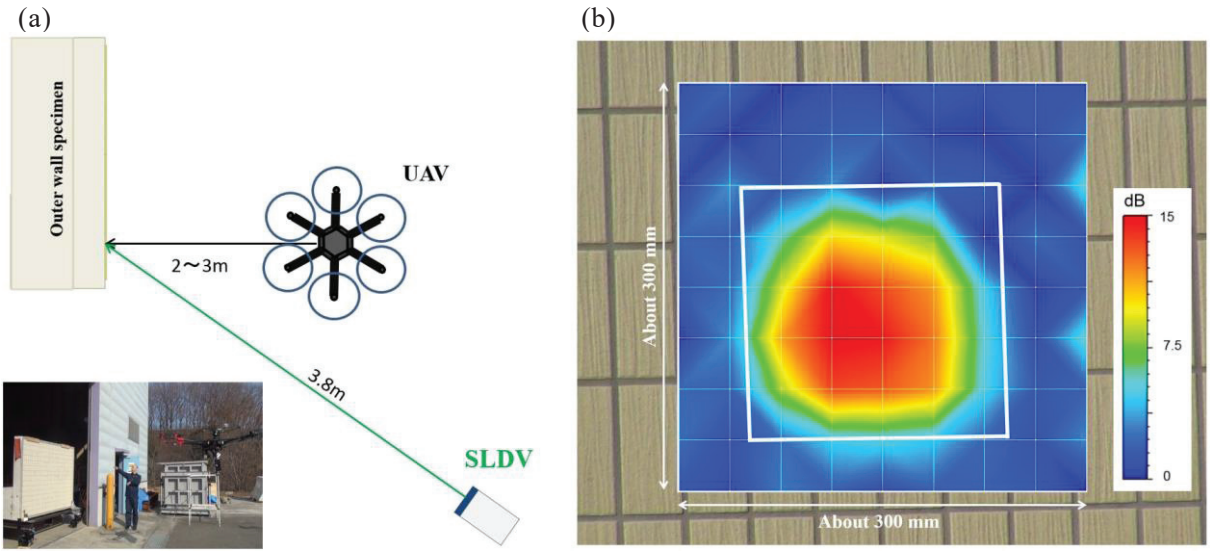

Figure 5 –Experiment when the acoustic wave is irradiated during UAV flight at very low attitudes. (a) Experimental setup, (b) An example of the experimental result using vibrational energy ratio (500-2400Hz). The measured object was a 200 mm^2 styrene sheet placed on the upper left of the specimen.

3.4 Experiment IV

3.4.1 Experimental setup

The large UAV was somewhat unstable at very low altitudes about the height of the specimen due to the wind generated by its own propeller. Then, the experiment at the time of UAV flight was carried out by lifting and arranging the outer wall specimen itself on another concrete specimen (3 m in height) using a large crane vehicle. Figure 6 (a) shows the experimental setup for UAV flight. At the time of the experiment, the sound source mounted UAV was manually operated so as to make it face substantially at the center of the specimen. Although the distance to the tile surface was controlled to be in the range of about 3 to 5 m, this distance is not constant because the position of the UAV swings occasionally due to the influence of the wind blowing. As seen from the SLDV (Polytec Corp., PSV-500 Xtra), the specimens were obliquely angled upward at an angle of about 26.7° and at a distance of about 11.2 m. The waveform used for acoustic irradiation induced vibration was a MTNB wave, and a waveform with an overall waveform length of 60 ms was used with a frequency range of 0.5 to 4 kHz and a pulse length of 3 ms (modulation frequency of 100 Hz). Also, the sound pressure is set

to about 90 dB (maximum value of Z characteristic) at 5 m distance.

3.4.2 Experimental result

The size of the measurement area was about 1.4 × 1.7 m^2, and measurements of 525 points (21 × 25) were performed at intervals of about 70 mm. Figure 6 (b) shows an example of the image results by vibration energy ratio. The frequency range for calculating the vibrational energy ratio was 0.9 to 4 kHz in accordance with the flexural resonance frequency of the size 100 to 200 mm^2 of the simulated defect. From the figure, it can be seen that 200 mm^2 for the styrene sheet and 150 mm^2 and 200 mm^2 for the foamed sheet are clearly detected. The following three points are considered to be the reason why 100 mm^2 and 150 mm^2 of the styrene sheet and 100 mm^2 of the foamed sheet were not detected.

・The sound pressure at the time of measurement was a little lower compared to indoor experiments.

・The number of measurement points was about half that of the indoor experiment (1015 points).

・The position of the UAV was not stable due to the influence of the wind, and accurate acoustic irradiation could not be performed on the defect part (The smaller the defect, the higher the resonant frequency, so the UAV position becomes important because of the directivity of the sound source).

Since averaging was not performed, the measurement time was about 137 seconds (This means that the measurement is 0.26 seconds per point). In addition, since the 50 mm^2 defect has a high flexural resonance frequency of 10 kHz or more, it was excluded from measurement this time.

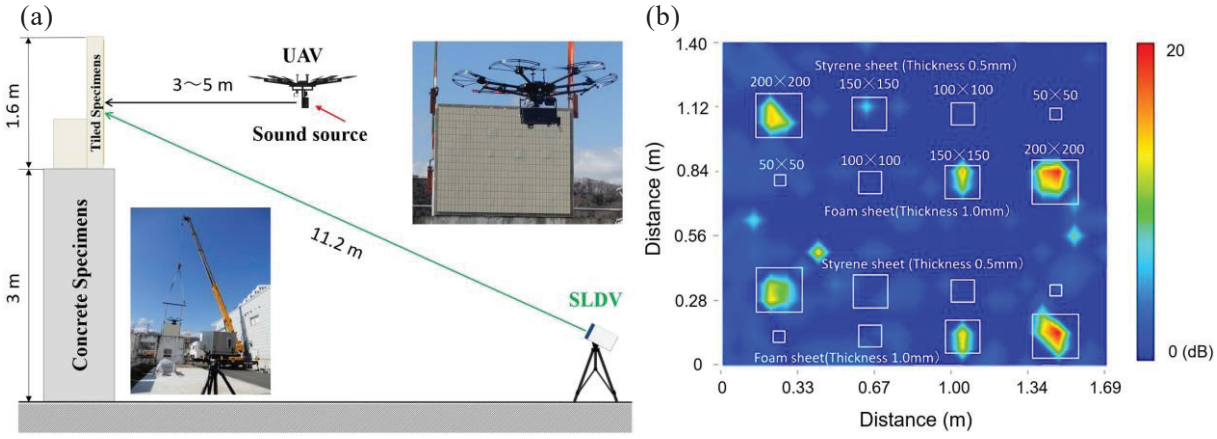

Figure 6 –Experiment when the acoustic wave is irradiated during UAV flight at about 4m height. (a) Experimental setup, (b) An example of the experimental result using vibrational energy ratio (900-4000Hz).

4. CONCLUSIONS

An UAV equipped with a flat speaker and a tiled outer wall specimen buried with thin sheets simulating crack defects were fabricated and fundamental experiments were conducted to check whether outer wall tiles can be inspected using the acoustic irradiation induced vibration from UAV. Experimental results proved that it is possible to detect crack defect of outer wall tile by the NCAI method using flexural resonance even for small sound source that can be mounted on UAV. Moreover, even if the UAV itself sways due to the influence of the wind, it was confirmed that the defect can be detected if the defect is within the directivity range of the sound source. Especially, since the position of the sound source and the high-sensitivity LDV are separated from each other, the influence of resonance of the laser head can be avoided, and it was also found that extremely high-speed measurement is possible. However, in order to use this method for actual outer wall inspection, there are many problems to be overcome, such as autonomous flight independent of GPS and automatic measurement in cooperation with LDV. Therefore, we will continue to consider practical application of this method in the future.

ACKNOWLEDGEMENTS

This work was supported by MLIT (Japan's Ministry of Land, Infrastructure, Transport and Tourism) Grant of Construction Technology R & D (2017-2018) and JSPS KAKENHI Grant Number JP17K12991.

REFERENCES

1. Sansalone MJ, Streett WB. Impact-Echo. Nondestructive evaluation of concrete and masonry. New York, USA: Bullbrier Press; 1997.
2. Cheng C, Sansalone MJ. The impact-echo response of concrete plates containing delaminations: numerical, experimental and field studies. Materials and Structures; 1993; 26(5): p.274-285.
3. Gericke OR. Determination of the geometry of hidden defects by ultrasonic pulse analysis testing, J. Acoust. Soc. Am. 1963; 35(3): 364-368.
4. Miyamoto R, Mizutani K, Ebihara T, Wakatsuki N. Effect of mode conversion of defect detection and size estimation in billet from time-of-flight profile by ultrasonic transmission method. Jpn. J. Appl. Phys. 2016; 55: 07KC06.
5. Tanaka S. Detection of Cracks and Air-gaps in Reinforced Concrete Structures Using an Electromagnetic Wave (Radar). Transactions of SICE. 2007; 43(9): p.716-724.
6. Kitagawa S, Kimura, S, Moriyama M, Utagawa N. Estimation of the deterioration for highway bridge RC slab by impact acoustics method. Life-Cycle of Structural Systems. Leiden, Holland: CRC Press/Belkema. 2015; p.2090-2096.
7. Mori K, Spagnoli A, Murakami Y, Kondo G, Torigoe I. A new non-contacting non destructive testing method for defect detection in concrete. NDT&E Int. 2002; 35: p.399-406.
8. Mori K, Tokuomi S. Nondestructive testing method for concrete structures by using water jet. Proc. JSME/ASME 2017 Int. Conf. Mater. Processing 2017; ICMP2017-4392.
9. Clark MR, McCann DM, Forde MC. Application of infrared thermography to the non-destructive testing of concrete and masonry bridges. NDT&E International 2003; 36(4): p. 265-275.
10. Shimada Y, Kotyaev O, Industrial Application Laser Remote Sens. Sharjah, United Arab Emirates: Bentham Science Publishers; 2012; Chap.9.
11. Osumi A, Ogita M, Okitsu K, Ito Y. Detection of crack in a shallow layer of mortar by using a harmonic component of very high intensity aerial ultrasonic waves. Jpn. J. Appl. Phys. 2017; 56: 07JC12.
12. Akamatsu R, Sugimoto T, Utagawa N, Katakura K. Proposal of non-contact inspection method for concrete structures, using high-power directional sound source and scanning laser Doppler vibrometer. Jpn. J. Appl. Phys. 2013; 52: 07HC12.
13. Akamatsu R, Sugimoto T, Utagawa N, Katakura K. Study on Non contact acoustic imaging method for concrete structures - Improvement of signal-to-noise ratio by using tone burst wave method. Proc. IEEE Int. Ultrasonic Symp. 2013; pp.1303-1306.
14. Katakura K, Akamatsu R, Sugimoto T, Utagawa N. Study on detectable size and depth of defects in noncontact acoustic inspection method. Jpn. J. Appl. Phys. 2014; 53: 07KC15.
15. Sugimoto K, Akamatsu R, Sugimoto T, Utagawa N, Kuroda C, Katakura K. Defect-detection algorithm for noncontact acoustic inspection using spectrum entropy. Jpn. J. Appl. Phys. 2015; 54: 07HC15.
16. Sugimoto K, Sugimoto T, Utagawa N, Kuroda C, Kawakami A. Detection of internal defects of concrete structures based on statistical evaluation of healthy part of concrete by noncontact acoustic inspection method. Jpn. J. Appl. Phys. 2018; 57: 07LC13.
17. Sugimoto T, Sugimoto K, Utagawa N, Katakura K. High-speed noncontact acoustic inspection method for civil engineering structure using multitone burst wave. Jpn. J. Appl. Phys. 2017; 56: 07JC10.
18. Sugimoto K, Sugimoto T, Utagawa N, Kuroda C. Detection of resonance frequency of both the internal defects of concrete and the laser head of laser Doppler vibrometer by spatial spectral entropy for noncontact acoustic inspection. Jpn. J. Appl. Phys. 2019; 58: (to be published).
19. Sugimoto T, Sugimoto K, Uechi I, Ohdaira T, Kawakami A, Utagawa N. Long distance measurement over 30m by high-speed noncontact acoustic inspection method using acoustic irradiation induced vibration. Proc. IEEE Int. Ultrasonic Symp. 2017; 6F-1.
20. Sugimoto T, Sugimoto K. Study on applicability of noncontact acoustic inspection method to shotcrete with rough surface. Proc. 12th European Conference for Non-Destructive Testing (ENCDT) 2018; ECNDT-561.
21. Sugimoto T, Sugimoto K, Utagawa N, Kuroda C, Kaneko T, Morioka H, Siki J, Nakagawa T. Defect detection of shotcrete with rough surface by noncontact acoustic inspection method. Proc. 6th Japan-US NDT Symp. 2018; 501037.
22. Dunford R, Michel K, Gagnage M, Piegay H, Tremelo ML. Potential and constraints of unmanned aerial vehicle technology for the characterization of mediterranean riparian forest. Int. J. Remote Sens. 2009; 30: p.4915-4935.